Muon spin relaxation in the spin-ring system Cu_3WO_6: Quasistatic spin freezing at 7.0 K

Y. Fudamoto,* I. M. Gat, M. I. Larkin, J. Merrin, B. Nachumi, A. T. Savici, and Y. J. Uemura
Department of Physics, Columbia University, New York, New York 10027

G. M. Luke
Department of Physics and Astronomy, McMaster University, Hamilton, Ontario, Canada L8S 4N1

K. M. Kojima
Department of Superconductivity, The University of Tokyo, Bunkyo-ku, Tokyo 113-8656, Japan

M. Hase
National Institute of Materials Science, Tsukuba, Ibaraki 305-0047, Japan

T. Masuda and K. Uchinokura
Department of Advanced Materials Sciences, The University of Tokyo, Bunkyo-ku, Tokyo 113-8656, Japan
(Received 6 November 2001; revised manuscript received 6 March 2002; published 8 May 2002)

Quasistatic spin freezing is observed at $T=7.0$ K in the muon spin relaxation (μSR) measurements of polycrystalline Cu_3WO_6. This material has been widely considered to possess a nonmagnetic spin-singlet ground state based on the previous neutron scattering and susceptibility studies in which a spin gap was observed. Zn-doped $Cu_{3-x}Zn_xWO_6$ with $x>0$, however, exhibit no signature of spin freezing. The μSR results of $Cu_{3-x}Zn_xWO_6$ are similar to those of a charge-ordered system $Na_xV_2O_5$. A few interpretations of the observed spin freezing will be presented.

DOI: 10.1103/PhysRevB.65.174428 PACS number(s): 75.40.Cx, 76.75.+i

I. INTRODUCTION

Spin gap systems have become a recent topical subject in studies of strongly correlated charge/spin systems. Quasi-one-dimensional spin systems often have spin-singlet ground states associated with the formation of a spin gap. Such systems include spin-Peierls $CuGeO_3$,[1] spin ladder $SrCu_2O_3$,[2] Haldane Y_2BaNiO_5,[3] and charge-ordered NaV_2O_5.[4] Magnetic dilution or charge doping with a very small amount of impurity substitution turns out to destroy the singlet ground state, and in some cases, leads to a long-range magnetic order as in $(Cu,Zn)GeO_3$ (Refs. 5,6) and $Sr(Cu,Zn)_2O_3$ (Ref. 7) or even to superconductivity as in $(Sr,Ca)_{14}Cu_{24}O_{41+\delta}$.[8] Doping effects in spin-gap systems have recently garnered additional interest since the existence of a pseudogap, which appears in the underdoped region of high-T_c cuprates, seems to be closely related to the appearance of superconductivity.

Cu_3WO_6 is a spin-gap system which contains magnetic rings consisting of six $S=1/2$ nearest-neighbor spins coupled antiferromagnetically. The crystal structure of Cu_3WO_6 has a cubic unit cell with space group $Pa\bar{3}$-T_h^6 and lattice constant $a=9.79$ Å.[9] It consists of distorted WO_6 octahedra and CuO_5 triangular bipyramids, in which only a Cu^{2+} ion (located inside the bipyramid) has a localized spin ($S=1/2$). Each CuO_5 bipyramid shares an edge with two other bipyramids and a corner with four other bipyramids. Six adjacent edge-sharing bipyramids then form a ring as shown in Fig. 1. The distance between two Cu^{2+} ions located in two edge-sharing bipyramids is 2.99 Å, while the distance in two corner-sharing bipyramids is 3.22 or 3.53 Å. It is considered that the edge sharing interaction is significantly stronger than the corner-sharing ones. This would lead to the dominant nearest-neighbor coupling of six $S=1/2$ Cu^{2+} spins to form a spin ring. These six-spin rings, however, are not isolated perfectly since Cu^{2+} ions in a ring are also coupled with those in other rings by the corner-sharing coupling.

The magnetic susceptibility of polycrystalline Cu_3WO_6 exhibits a sharp reduction at low temperatures, indicating the existence of the singlet ground state with a gap energy $\Delta=110$ K.[10] At high temperatures, the experimental value of the susceptibility is much lower than a theoretical value:[11] about 2/3 lower around the maximum at $T\sim 130$ K. This reduction of the susceptibility has been discussed in terms of a possible resonating valence bond (RVB) state.[10]

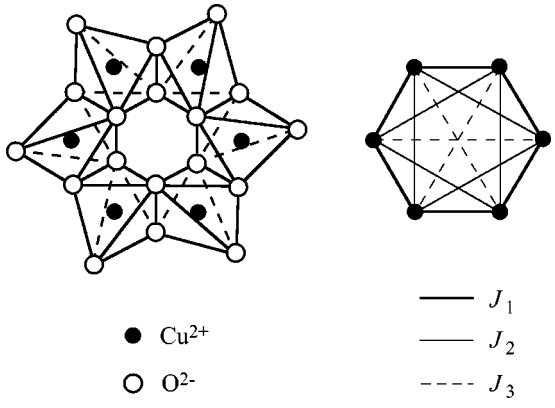

FIG. 1. (Left) A six-spin ring in Cu_3WO_6, formed by CuO_5 bipyramids. Solid and open circles represent Cu^{2+} and O^{2-} ions, respectively. Cu^{2+} ions in the ring are coupled by the nearest-neighbor interactions. (Right) The first (J_1), the second (J_2) and the third (J_3) nearest-neighbor interactions within the ring.

In inelastic neutron scattering measurements,[12] two peaks at 11 and 14 meV were observed in constant-Q energy spectra. In theoretical calculations of the singlet-triplet excitations, these peak values can be reproduced for $J_2/J_1=0.64$ and $J_3/J_1=0.51$, where J_1, J_2, and J_3 are the first, second, and third nearest-neighbor antiferromagnetic superexchange interactions, respectively, within the ring (Fig. 1). Note that J_1 is equivalent to the edge-sharing coupling mentioned above, but J_2 and J_3 are different from the two corner-sharing couplings. However, the observed susceptibility curves could not be reproduced assuming these values of the superexchange couplings. This feature was ascribed in Ref. 12 to the existence of interring corner-sharing interactions.

In this paper, we report muon spin relaxation (μSR) and magnetic susceptibility measurements of polycrystalline $Cu_{3-x}Zn_xWO_6$. Muon spin relaxation is a powerful magnetic probe to study static and dynamic magnetism. It has the capability to detect magnetic moments as small as $\sim 0.01\mu_B$ and dynamic fluctuation rates in a rather large time window ranging between $10^7 \sim 10^{12}$ s^{-1}. We have observed quasistatic spin freezing at $T=7.0$ K in pure Cu_3WO_6. In Zn-doped $Cu_{3-x}Zn_xWO_6$ with $x=0.01$, 0.05, and 0.10, however, no spin freezing is observed down to $T=2.20$, 0.10, and 0.10 K, respectively. We discuss similarities between the μSR results of $Cu_{3-x}Zn_xWO_6$ and those of a charge-ordered system $Na_xV_2O_5$ and other widely accepted spin-gap systems. A few possible interpretations of the observed spin freezing will also be provided.

II. EXPERIMENTAL PROCEDURE

A. Sample preparation and characterization

Polycrystalline samples of $Cu_{3-x}Zn_xWO_6$ were produced by the solid state reaction method. Mixtures of CuO, ZnO, and WO_3 with an appropriate molar ratio were pressed into pellets and heated at 800 °C in an evacuated silica tube for several days with some intermediate grindings. Although a diffraction pattern of $CuWO_{4-x}$ is detected in the x-ray diffraction measurements for all specimens, the intensity of this impurity phase remains very weak and has no correlation with x.

Using a SQUID magnetometer, we measured the magnetic susceptibility of the specimens used in the present μSR study. Figure 2 shows the results obtained in applied external field of 50 G. The susceptibility $\chi(T)$ of both the undoped and the doped specimens exhibits the Curie (1/T) type increase at low temperatures, which indicates the existence of dilute free spins. $\chi(T)$ at low temperatures are fit with

$$\chi(T)=\frac{C}{T-\theta}+A\exp\left(-\frac{\Delta}{T}\right)+K, \qquad (1)$$

where the first term represents the Curie-Weiss behavior due to free spins, the second term represents the gap excitation, and the third term is a constant. Table I is the list of parameters obtained from the best fit. The numbers of impurities calculated from the Curie term for the case of $S=1/2$ free spins are also included in Table I and denoted as % impurity per Cu atom. These % impurities for the Zn-doped specimen show a fairly good agreement with the Zn doping concentrations, corresponding to x/3.00 in Table I. This verifies that the Curie term originates predominantly from $S=1/2$ spin, each created by one (Cu,Zn) substitution. The Curie-Weiss form is used, rather than the Curie form (C/T), to obtain better results in the fitting, but the magnitudes of θ remain smaller than the lowest temperature limit of 2.0 K in the measurements. Note the susceptibility shows no hysteresis in field-cooling–zero-field-cooling processes.

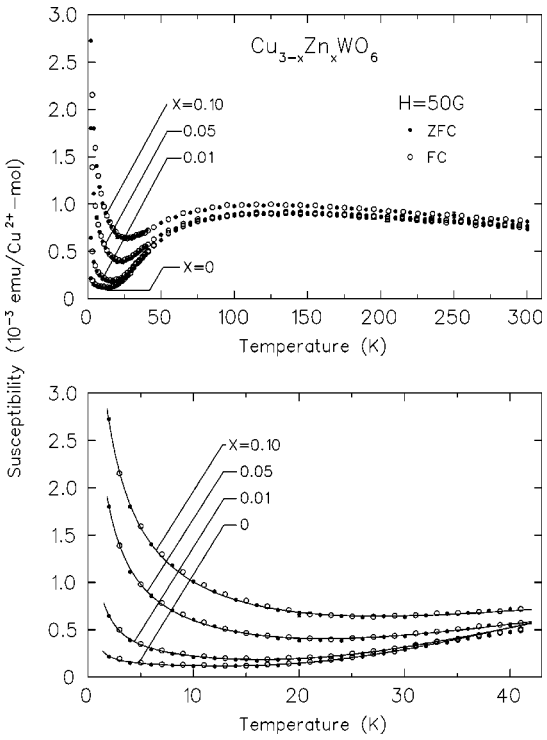

FIG. 2. Susceptibility of polycrystalline $Cu_{3-x}Zn_xWO_6$ ($x=0$, 0.01, 0.05, and 0.10) specimens used for the present μSR study. Open and closed circles indicate values obtained in field-cooling and zero-field-cooling processes, respectively. Solid lines represent Eq. (1).

B. Muon spin relaxation technique

Muon spin relaxation measurements of Cu_3WO_6 were performed at the $M13$ and $M15$ muon channels at TRIUMF. Several pieces of polycrystalline $Cu_{3-x}Zn_xWO_6$ were placed on a thin silver plate, and then wrapped with silver or aluminum foil. The samples were mounted in a He-flow cryostat and a dilution refrigerator for measurements down to 2.0 and 0.10 K, respectively. Positive muons were implanted in the specimen with their spin polarized parallel to the beam direction. Muons undergo Larmor precession due to the internal magnetic field $H_{\rm int}$ with an angular frequency $\omega=\gamma_\mu H_{\rm int}$, where γ_μ is the gyromagnetic ratio of $2\pi\times 13.554$ MHz/kG. After precessing during time t, each muon decays into a positron and two neutrinos. Time histograms $F(t)$ and $B(t)$ of muon-decay positrons are recorded by two sets of counters placed forward and backward of specimen with respect to the initial muon spin direction. Due to the parity violation of the weak interaction, positrons are

TABLE I. List of parameters obtained from the best fit of the susceptibility (Fig. 2) to Eq. (1) at low temperatures.

x	$C\times10^{-4}$ [a]	θ (K)	$A\times10^{-3}$ [a]	Δ (K)	$K\times10^{-5}$ [a]	% impurity	x/3.00 (%)
0	2.49	0	4.70	96.5	9.52	0.0663	0
0.01	14.0	-0.51	4.17	93.9	8.81	0.373	0.33
0.05	52.2	-1.14	2.67	87.3	12.9	1.39	1.66
0.10	88.3	-1.61	1.91	82.6	24.4	2.35	3.33

[a]In units of (emu/Cu^{2+} mol).

emitted preferentially along the muon spin direction. Thus, the counting rates are given as

$$F'(t)\propto[1+A(t)]\exp\left(-\frac{t}{\tau_\mu}\right) \tag{2}$$

and

$$B'(t)\propto[1-A(t)]\exp\left(-\frac{t}{\tau_\mu}\right), \tag{3}$$

where $F'(t)$ and $B'(t)$ indicate background-subtracted histograms, τ_μ is the muon lifetime of 2.2 μs, and $A(t)$ is an asymmetry due to Larmor precessions of muons in the internal field. Time evolution of the muon-decay asymmetry $A(t)$ can then be directly obtained, after normalizing solid angle factors for the forward and backward counters, as

$$A(t)=\frac{F'(t)-B'(t)}{F'(t)+B'(t)}. \tag{4}$$

$A(t)$ can be compared with a theoretical muon spin relaxation function $G_z(t)$.

C. Relaxation functions in various situations

$G_z(t)$ for Gaussian (called the Kubo-Toyabe function), Lorentzian and some other distributions of random local fields have been described in Refs. 13,14. As an example, we show static relaxation functions for the Lorentzian field distribution in Fig. 3(a). (Below we will analyze the μSR data of Cu_3WO_6 with these functions.) The Lorentzian distribution of internal field components is given by $P(H_i)=(\gamma_\mu/\pi)\times[a/(a^2+\gamma_\mu^2H_i^2)]$ $(i=x,y,z)$, where a is the half-width half-maximum of the distribution, and can be constructed assuming random freezing of dilute spins. The static relaxation function for the Lorentzian field distribution in zero external field (ZF) is given by

$$G^L(a,t)=\frac{1}{3}+\frac{2}{3}(1-at)\exp(-at), \tag{5}$$

which is characterized by damping of the 2/3 of the asymmetry at early times and the persistence of the 1/3 component in the long time limit. Figure 3(a) also shows the dependence of the relaxation function on H_L, the external longitudinal field (LF) which is applied parallel to the initial muon spin direction. The 1/3 component in ZF is raised in the applied LF, and approaches to 1 as $\gamma_\mu H_L/a\rightarrow\infty$.

In the paramagnetic phase of ordinary magnetic systems, the total amplitude of each spin S undergoes completely random fluctuations as illustrated in Fig. 4(a), which lead to fluctuations of the local magnetic field at the muon site with the full amplitude. Figure 3(b) shows the relaxation function $G(t)$ expected in these paramagnetic fluctuations in dilute spin systems which give a Lorentzian field distribution at muon sites.[14] Dynamic fluctuations with slow fluctuation rate $\nu/a<1$ are reflected in the slow decay of the 1/3 component. The polarization minimum disappears as $\nu\sim a$. One sees the reduction of the depolarization rate (corresponding to the narrowing effect in terms of magnetic resonance) in the fast fluctuation limit $\nu/a\gg1$. In this limit $G_z(t)$ has the shape of stretched exponential function $\exp[-(\lambda t)^\beta]$ with the power $\beta=0.5$.[14]

In the ordered state of magnetic systems, each spin S acquires two components, i.e., the effectively static component

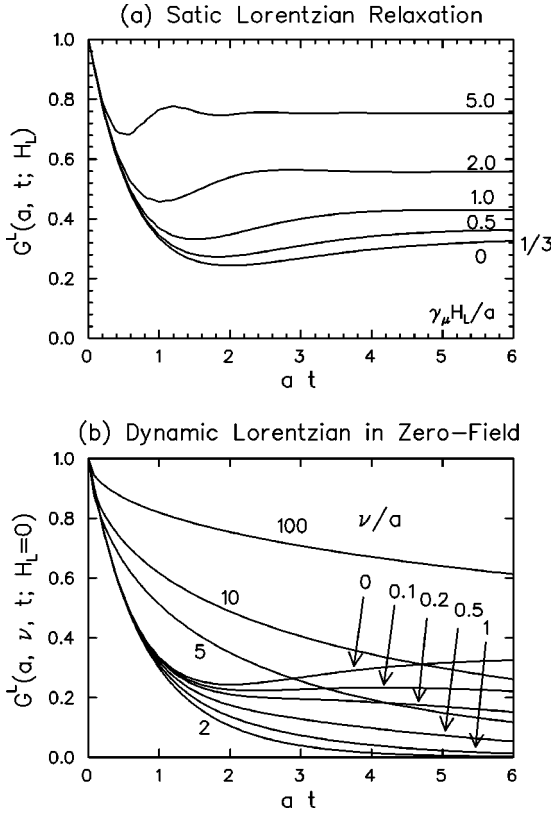

FIG. 3. Static muon spin relaxation functions for the Lorentzian field distributions. (a) In zero external field and applied longitudinal fields and (b) with dynamic fluctuations.

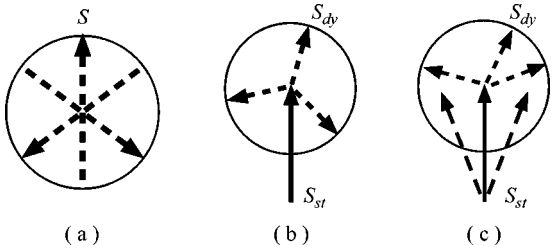

FIG. 4. Schematic illustration of various models of spin fluctuations. (a) In the paramagnetic phase, total amplitude of each spin S undergoes random fluctuations. (b) In the quasistatic phase, spins (S) are divided into static ($S_{\rm st}$) and dynamic ($S_{\rm dy}$) components, such that $S^2=S_{\rm st}^2+S_{\rm dy}^2$. (c) Static components $S_{\rm st}$ are also assumed to be fluctuating slowly.

$S_{\rm st}$, and dynamic component $S_{\rm dy}$, as illustrated in Fig. 4(b). In neutron scattering, the static component shows up as the intensity of Bragg reflection. Below the Curie or Néel temperature (T_c or T_N), the static component increases with decreasing temperature, as shown by the temperature dependence of the elastic Bragg peak intensity $I_B \propto S_{\rm st}^2$.

The dynamic component is due to thermal and/or quantum spin fluctuations, which originate from various phenomena, such as spin wave excitations, excitations above a spin gap, etc. The energy-integrated intensity of inelastic neutron scattering, i.e., the intensity $I_{\rm da}$ observed in the so-called double-axis configuration, is proportional to the instantaneous spin value S^2. If we define $S_{\rm dy}^2$ to be proportional to the truly inelastic intensity $(I_{\rm da}-I_B)$, then it is most natural to assume $S^2=S_{\rm st}^2+S_{\rm dy}^2$.

Coexisting $S_{\rm st}$ and $S_{\rm dy}$ would make coexisting static and dynamic components $H_{\rm st}$ and $H_{\rm dy}$ in the local field $H_{\rm loc}$ at the muon site. When the fluctuation rate ν of $H_{\rm dy}$ is much larger than the difference of the Zeeman levels of the muon spin due to static external field H_L and/or internal field $H_{\rm st}$, i.e., $\nu \gg \gamma_\mu H_L$ and $\nu \gg \gamma_\mu H_{\rm st}$, then $H_{\rm st}$ and $H_{\rm dy}$ contribute independently to depolarization of muon spins. In this case the relaxation function at each muon site becomes a product of the static relaxation function $G_{\rm st}(t)$ for $H_{\rm st}$ and the dynamic relaxation function $G_{\rm dy}(t)$ for $H_{\rm dy}$. The simplest example for this is a polycrystalline sample of a system in which every muon site has the same local field $H_{\rm loc}$ without distribution. In this case, $G(t)=G_{\rm st}(t)\times G_{\rm dy}(t)$, where $G_{\rm st}(t)=(1/3)+(2/3)\cos(\omega t)$ with $\omega=\gamma_\mu H_{\rm st}$ represents the muon spin precession around $H_{\rm st}$, while $G_{\rm dy}(t)=\exp(-t/T_1)$ represents the T_1 process as $1/T_1 \sim (\gamma_\mu H_{\rm dy})^2/\nu$.

One can extend this treatment to calculate $G(t)$ for systems having a Gaussian distribution of H by using the Kubo-Toyabe function for $G_{\rm st}(t)$. For the case of systems which involve muon sites with inequivalent field amplitudes, one has to calculate $G(t)$ for each site first, and then obtain the site average afterwards, as described in Ref. 14. For the Lorentzian distribution, this situation of coexisting $H_{\rm st}$ and $H_{\rm dy}$ can be expressed with three parameters $a_{\rm st}$, $a_{\rm dy}$, and ν, where $a_{\rm st}$ and $a_{\rm dy}$ represent the (half-width at half maximum) amplitudes of the static and dynamic Lorentzian field distributions, respectively. With site-averaged static and dynamic fields, the treatment $G(t)=G_{\rm st}(t)\times G_{\rm dy}(t)$ is no longer strictly correct, but does provide a good parametrization of $a_{\rm st}$, $a_{\rm dy}$, and ν in the limit of $a_{\rm st} \gg a_{\rm dy}^2/\nu$. $G_{\rm st}(t)$ and $G_{\rm dy}(t)$, in the limit of fast dynamic fluctuations $\nu/a_{\rm dy} \gg 1$, are given by[14]

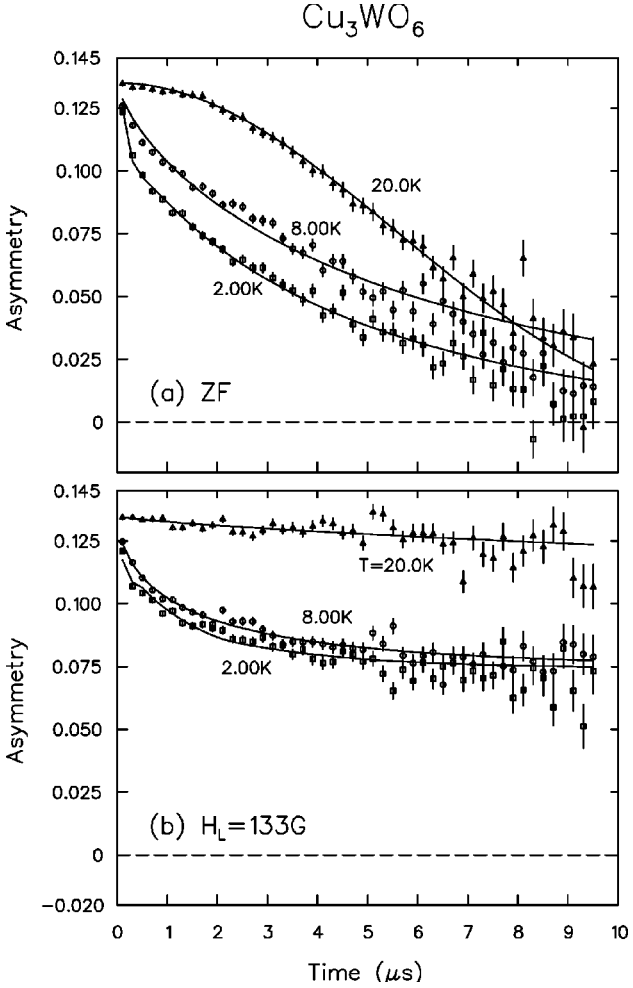

FIG. 5. μSR spectra of polycrystalline Cu_3WO_6 (a) in zero external field and (b) in the longitudinal field $H_L=133$ G. Solid lines are guides to the eye.

$$G_{\rm st}(t)=\frac{1}{3}+\frac{2}{3}(1-a_{\rm st}t)\exp(-a_{\rm st}t) \tag{6}$$

and

$$G_{\rm dy}(t)=\exp[-(4a_{\rm dy}^2 t/\nu)^{0.5}]. \tag{7}$$

III. RESULTS AND ANALYSIS OF Cu_3WO_6

A. Two different magnetic environments

Figure 5(a) shows time spectra of the muon spin polarization in polycrystalline Cu_3WO_6 in zero external field (ZF). Below $T=7.0$ K, fast reduction of the muon spin polarization is observed at early time $t<0.4$ μs, followed by slow depolarization in a longer time range. The depolarization becomes slower with increasing temperatures, and the fast depolarization is no longer observed above 7.0 K. In the mod-

erately high longitudinal field of $H_L=133$ G, the slow depolarization is almost completely suppressed [Fig. 5(b)] at any temperature, while about a half of the total asymmetry still exhibits depolarization, which becomes slower gradually with increasing temperature. These features indicate the existence of two different magnetic environments for muons.

The LF dependence of the slower component confirms that the depolarization for this component is due to a small static internal field. There exists small random static fields created by nuclear dipoles μ_N ($\sim\mu_B/1000$) throughout the entire temperature range. The slow depolarization could be attributed to these nuclear dipoles. However, this depolarization is so slow that it is hard to determine the shape of the spectra, and consequently the origin of the depolarization. Likely reasons for the existence of such muon sites with almost no internal field could be: (a) Cu spins are divided into inactive spin-singlet pairs and active unpaired spins, and a spatial distribution of regions are created by these kinds of spins, leading to a partial volume fraction with active internal fields from the unpaired spins at muon sites and/or (b) the internal field at some muon sites are cancelled due to crystal symmetry with respect to surrounding Cu moments. Experimentally, we can obtain almost no information from these low/zero-field muon sites. Therefore, in the following description, we limit our discussion only to the fast depolarization of the signal, which is due to muon sites with active internal magnetic fields.

The effect of nuclear dipolar fields in the spectrum of the component with the fast depolarization becomes dominant above $T=20$ K in ZF, as indicated by the Gaussian relaxation of the entire asymmetry. A small longitudinal field $H_L=133$ G eliminates this depolarization at 20 K, confirming that this depolarization is caused by a small static field. In Fig. 6(a), we show the spectra in $H_L=133$ G at early times. This field is sufficiently high to suppress the depolarization due to the zero/low-field muon sites, as well as the depolarization due to nuclear dipoles in the fast-depolarization component. Therefore, the observed depolarization in $H_L=133$ G is purely electronic in origin.

The component with the fast depolarization shows substantial depolarization in $H_L=133$ G at any temperature, indicating the strong dynamic character of the electron spins. The dynamic fluctuations of the electron moments persist even at $T\sim 2.0$ K. The longitudinal field dependence of the spectra at $T=2.0$ K [Fig. 6(b)] exhibits a characteristic feature of depolarization caused by quasistatic fields with $\nu/a \leqslant 1$. This quasistatic field is decoupled by longitudinal fields (LF's) of 133 G$<H_L<1$ kG. The magnitude of the internal field estimated from this decoupling is $H_{\rm int}\sim 30$ G. There is, however, no sign of coherent oscillation of the muon spin polarization in zero field, indicating the broadness of the distribution of the local field.

The spectra in $H_L=133$ G below $T_f=7.0$ K have been analyzed with the function

$$A(t)=A_1G(t;H_L)+A_2, \tag{8}$$

where the first term represents the fast quasistatic/dynamic depolarization and the second term the decoupled full asymmetry due to the zero/low-field muon sites. We obtained $A_1=0.061$ as the experimental initial asymmetry of the fast depolarization component and $A_2=0.074$ for the slow component.

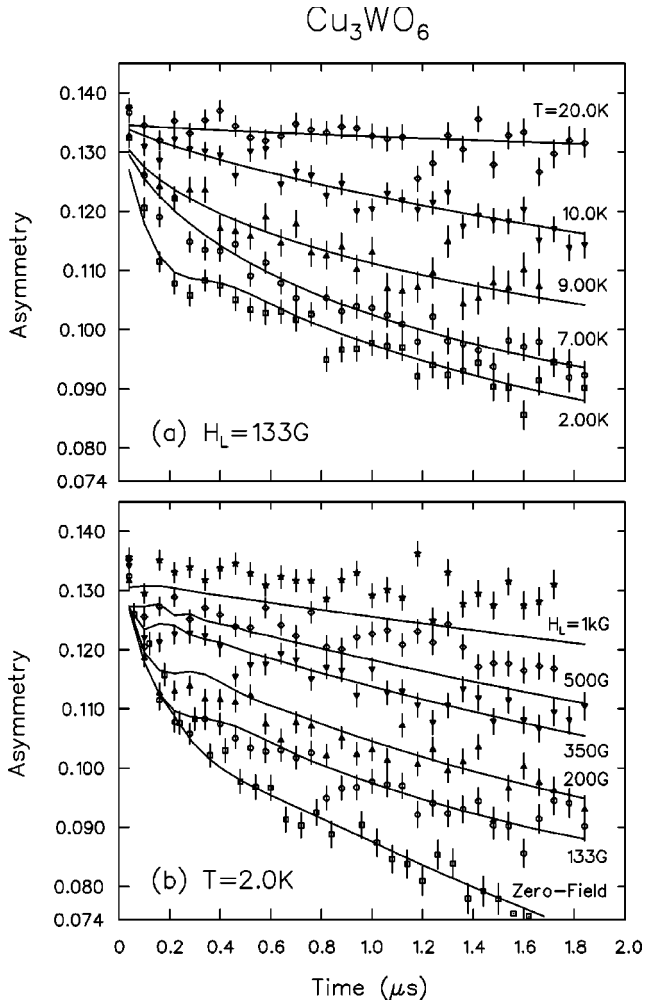

FIG. 6. (a) μSR spectra of polycrystalline Cu_3WO_6 in the longitudinal field $H_L=133$ G at early time. Solid lines represent the best fit to Eq. (8) below the freezing temperature $T_f=7.0$ K and Eq. (13) above T_f. (b) LF μSR spectra of polycrystalline Cu_3WO_6 at $T=2.0$ K. Solid lines correspond to Eq. 8, with fixed $a=2.85$ and $\nu=2.25$ μs^{-1} obtained from the best fit for the spectra at $T=2.0$ K. The spectra are decoupled approximately following the theoretical line shapes.

B. Results at $T=2.0$ K

In our first attempt to fit the results at $T=2.0$ K in various LF values, we assumed the model of coexisting static and fast dynamic local fields, both having Lorentzian distributions, with a single value of ν, and assumed $G(t)$ to be given by $G_{\rm st}(t;a_{\rm st},H_L)$ (Ref. 14) multiplied to $G_{\rm dy}(t)=\exp[-(\lambda t)^{0.5}]$, similarly to the case of $H_L=0$ given in Eqs. (6) and (7). Figure 7(a) compares the observed results of LF-μSR in Cu_3WO_6 with this model for $a_{\rm st}=2.0$ μs^{-1} with the values of λ at various H_L in Fig. 7(b). From the field dependence of λ, we obtain $a_{\rm dy}=1.7$ and $\nu=12.0$ μs^{-1}.

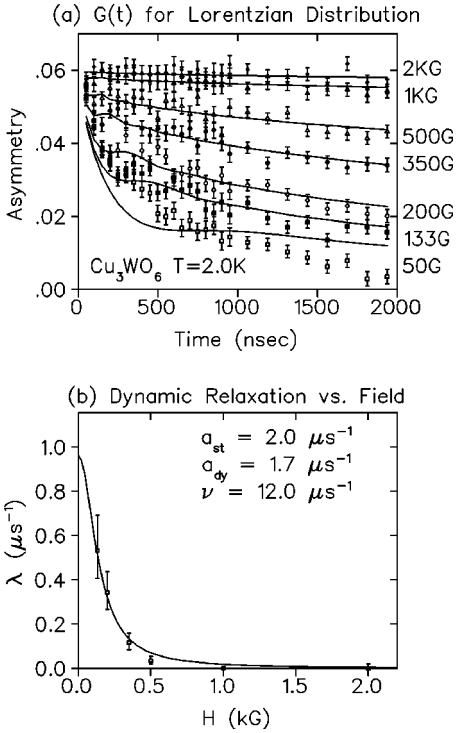

FIG. 7. (a) Fits to $A_1 G_{\rm st}(t) \times G_{\rm dy}(t)$ assuming Lorentzian distribution of fields. The asymmetry is shifted by $A_2 = 0.074$. (b) λ versus applied field H_L assuming Lorentzian distribution. Solid line represents $\lambda = 4a_{\rm dy}^2 \nu / [\nu^2 + (\gamma_\mu H_L)^2]$.

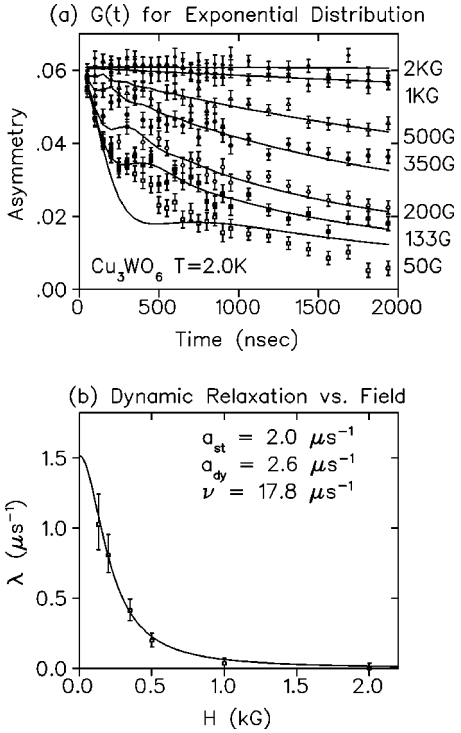

FIG. 8. (a) Fits to $A_1 G_{\rm st}(t) \times G_{\rm dy}(t)$ assuming exponential distribution of fields. The asymmetry is shifted by $A_2 = 0.074$. (b) λ versus applied field H_L assuming exponential distribution. Solid line represents $\lambda = 4\delta_{\rm dy}^2 \nu / [\nu^2 + (\gamma_\mu H_L)^2]$ (Ref. 17).

The full amplitude $a = [a_{\rm st}^2 + a_{\rm dy}^2]^{0.5}$ becomes 2.7 μs^{-1}. As shown in Fig. 7(a), this model reproduces well the observed decoupling by longitudinal external fields and the slow decay in a long time scale $t > 500$ ns at $H_L \geqslant 133$ G. However, this model gives too fast damping of the initial decay at early times $t < 200$ ns, presumably due to the sharp change of the square-root exponential dynamic function near $t \to 0$. It also fails to reproduce the moderate decay at $H_L = 50$ G observed around $t = 500$ ns.

To improve these difficulties, we next attempted fitting the data with an exponential distribution for the local field

$$P(H_i) = \frac{\gamma_\mu}{2\delta} e^{-\gamma_\mu |H_i|/\delta} \quad (i = x, y, z), \tag{9}$$

instead of Lorentzian distribution. The exponential field distribution has worked quite well for fitting the results of μSR in a Zn-doped two-leg ladder systems $Sr(Cu,Zn)_2O_3$,[15,16] a system where a small perturbation induces spin freezing in some volume of Cu moments, with the ordered moment size having a wide spatial variation, while the spin-gap feature still survives in inelastic neutron scattering studies.[18] The present system might have similar features, since its static order might be due to some perturbation to an otherwise complete spin-gap system. For this distribution, the static function is given as

$$G_{\rm st}(t) = \frac{1}{3} + \frac{2}{3}\left\{ \frac{1 - (\delta t)^2}{[1 + (\delta t)^2]^2} \right\}, \tag{10}$$

and the dynamic one as

$$G_{\rm dy}(t) = \frac{1}{1 + \lambda t}, \tag{11}$$

with $\lambda = 4\delta^2/\nu$.[17]

Figures 8(a) and 8(b) show the fit with this exponential field distribution, again using $G(t) = G_{\rm st}(t) \times G_{\rm dy}(t)$ with $\delta_{\rm st} = 3.0$ μs^{-1} to parametrize the coexistence of static and fast-dynamic field amplitudes. The field dependence of λ gives $\delta_{\rm dy} = 2.6$ μs^{-1} with the fluctuation rate $\nu = 18$ μs^{-1}.[17] Since the widths δ and a correspond to exponential and Lorentzian distributions, respectively, defined in the two different models, we can only make a crude comparison between the results. The model functions with an exponential field distribution reproduce the early-time initial damping rather well. For this distribution, the dynamic contribution $G_{\rm dy}(t)$ does not exhibit an overly sharp behavior near $t \to 0$. A difficulty still remains, however, regarding the moderate damping in $H_L = 50$ G at $t \sim 500$ ns.

As our third attempt, we tried to use the paramagnetic model with a Lorentzian field distribution. It is rather phenomenological to use this model for the results obtained below the spin freezing temperature. However, this model, if used with a as a temperature dependent parameter, can possibly cover quasistatic slow fluctuations of $S_{\rm st}$ and thus $H_{\rm st}$ with the time scale of $\nu \sim a_{\rm st}$. This situation is illustrated in Fig. 4(c).

Figure 6(b) shows the results of this attempt with $a = 2.85$ μs^{-1} and $\nu = 2.25$ μs^{-1}. Now the moderate relax-

ation in low fields around $t \sim 500$ ns is reproduced well. This suggests the strong effect of slow and quasistatic spin fluctuations with $\nu \sim a$ and also a possible wide distribution in the time scale ν of the local field fluctuations. All three analyses, however, indicated the existence of a quasistatic local field having an effective amplitude of $a/\gamma_\mu \sim 30$ G.

In general, one could even try different models by assuming that the moderate relaxation is due to additional muon sites having a different effective field amplitude. However, we consider that providing further freedom to data analyses will simply introduce too many assumptions, which can hardly be verified. Therefore, we shall proceed with the following analyses at $T > 2$ K, resorting to a simpler phenomenological procedure.

C. Results at $T > 2.0$ K

In the long-time limit in the magnetically frozen state, any function for coexisting static and dynamic depolarization can be approximated as $G(\lambda,t) \sim A_1' \exp[-(\lambda t)^\beta]$, where λ is the dynamic depolarization rate. The value of A_1' depends on the ratio $\gamma_\mu H_L/a$; A_1' takes the value 1/3 for the zero-field case, and approaches 1 as $\gamma_\mu H_L/a \to \infty$. The stretching power β has a value $\beta = 1/2$ for the case of spatially dilute spin systems (and $\beta = 1$ for dense spin systems) with a single dynamic fluctuation rate. β often takes different values in spin glass systems, reflecting a distribution of dynamic fluctuation rates. To obtain the dynamic depolarization, we therefore fit the spectra for $t > 0.5$ μs with the function

$$A(t) = A_1' \exp[-(\lambda t)^\beta] + A_2. \tag{12}$$

A_1' is left as a free parameter and β is allowed to vary in the range $\beta < 1.0$. In the paramagnetic phase, the depolarization is entirely due to the dynamic process of the electron spins. Above T_f, the LF spectra in $H_L = 133$ G are thus analyzed using

$$A(t) = A_1 \exp[-(\lambda t)^\beta] + A_2, \tag{13}$$

for the entire time range, with A_1 fixed to the previously given value of 0.061.

In high longitudinal field $H_L \geqslant 500$ G, the fast static depolarization at low temperatures is almost completely suppressed, and the persisting observed depolarization is due only to the dynamic processes of the electron spins. Thus, the spectra in $H_L = 500$ G are analyzed with Eq. (13) for the entire temperature range.

In order to account for the temperature dependence of the quasistatic internal field amplitude below the freezing temperature, we fitted the early time part of the observed spectra using the slowly fluctuating paramagnetic model and allowing temperature dependence of the parameter a. Although the actual instantaneous magnitude of the local field would not depend on temperature, the present fitting procedure allows us to obtain the magnitude of quasistatic local fields.

In Figs. 9(a), 9(b), and 9(c), we show temperature dependence of the quasistatic field amplitude a, the dynamic depolarization rate λ and the stretching exponent β obtained from the data analyses mentioned above. The sharp reduction of

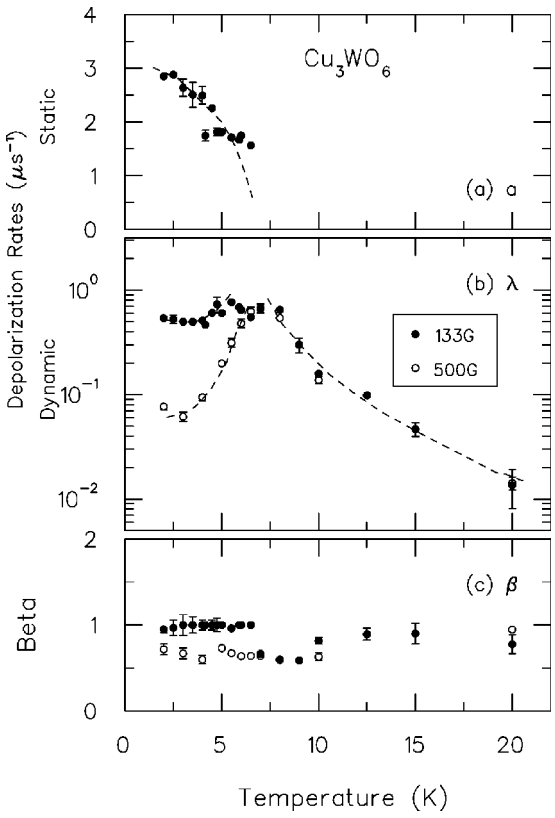

FIG. 9. Temperature dependences of (a) the static depolarization rate a, (b) the dynamic depolarization rate λ, and (c) the stretching exponent β, defined in Eqs. (8)–(13), in polycrystalline Cu_3WO_6. Broken lines are guides to the eye.

the quasistatic field amplitude a, divergence of the dynamic depolarization rate λ, and decrease of the stretching exponent β near the freezing temperature are all characteristic features of systems with random spin freezing. The static depolarization rate a gives the internal field at which the probability distribution of the field magnitude $P(|H|) = (\gamma_\mu^3/\pi^2) \times [a/(a^2 + \gamma_\mu^2 H^2)]^2 \times 4\pi H^2$ takes its maximum value, and $a = 2.85$ μs^{-1} at $T = 2.0$ K corresponds to the field of $H_{\max} = a/\gamma_\mu = 34.0$ G. We define this amplitude of the local field to be a_0.

D. Spin fluctuation in the paramagnetic state

We can estimate the fluctuation rate ν of the fluctuating moments in the paramagnetic phase $T > T_f$, assuming that the full-amplitude fluctuation of a_0 which leads to the relationship $\lambda = 4a_0^2/\nu$. Since the stretched exponential function with $\beta \ll 1.0$ has a very sharp reduction at early times, the depolarization rate λ resulting from the stretched exponential fit with the low β values tends to underestimate an average depolarization rate. In order to compensate this effect, we calculate $\lambda_{1/2} = 1/T_{1/2} = \lambda/\ln(2)^{1/\beta}$, where $T_{1/2}$ is the time for the muon polarization to drop to 1/2 of the initial value. To compare with the usually measured $1/T_1$, we use $\lambda^* = \lambda_{1/2} \ln(2)$. Figure 10 shows the the average fluctuation rate $\nu^* \sim a_0^2/\lambda^*$. Comparing with thermal activation behavior

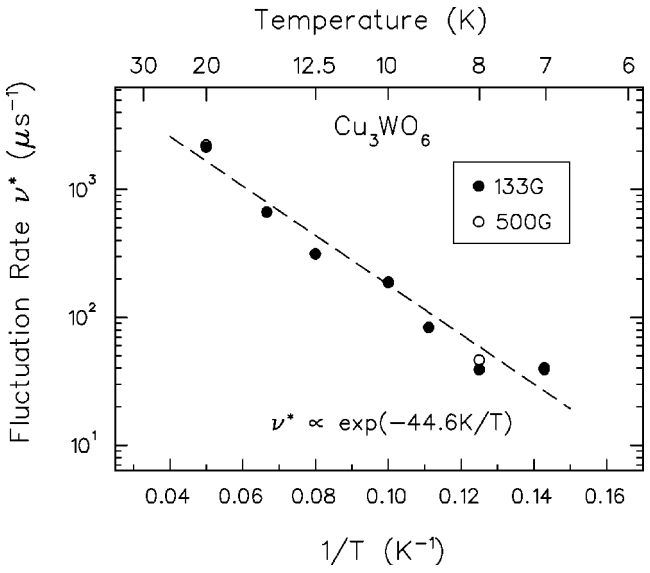

FIG. 10. Temperature dependence of the average fluctuation rate ν^* of the fluctuating local fields in polycrystalline Cu_3WO_6. The broken line corresponds to the thermal activation behavior [Eq. (14)].

$$\nu^* \propto \exp\left(-\frac{E_g}{k_B T}\right), \tag{14}$$

we obtain a gap energy $E_g = 44.6$ K, which is roughly half of the spin-gap energy $E_g \sim 110$ K obtained in susceptibility[10] and neutron measurements,[12] but much larger than the freezing temperature $T_f = 7.0$ K.

IV. SUPPRESSION OF SPIN FREEZING BY MAGNETIC DILUTIONS

Cu_3WO_6 can be magnetically diluted by substituting nonmagnetic Zn^{2+} (spin-0) for magnetic Cu^{2+} (spin-1/2) ions. In $Cu_{3-x}Zn_xWO_6$, a sharp reduction of the susceptibility towards $T \to 0$ is suppressed (Fig. 2), indicating the suppression of a spin-gap formation. Gap energy Δ decreased with increasing Zn concentration x (Table I).

Figure 11 shows ZF-μSR spectra of $Cu_{3-x}Zn_xWO_6$ with $x = 0.01$, 0.05, and 0.10 at low temperatures. The fast depolarization caused by nearly static electron spins observed in pure Cu_3WO_6 no longer exists, and only a slow depolarization due to nuclear dipoles are observed. A small amount of (Cu,Zn) substitution is thus enough to enhance the fluctuation of electron spins drastically and eliminate the quasistatic component.

The spectra are consistent with $A(t) = AG^G(\Delta_{\rm nucl}, t)$, where

$$G^G(\Delta_{\rm nucl}, t) = \frac{1}{3} + \frac{2}{3}(1 - \Delta_{\rm nucl}^2 t^2)\exp\left(-\frac{\Delta_{\rm nucl}^2 t^2}{2}\right) \tag{15}$$

is the Gaussian Kubo-Toyabe function, and $\Delta_{\rm nucl}$ is a static depolarization rate due to random local fields created by nuclear dipoles. Figure 12 shows the x dependence of the depolarization rate $\Delta_{\rm nucl}$. The depolarization rate remains

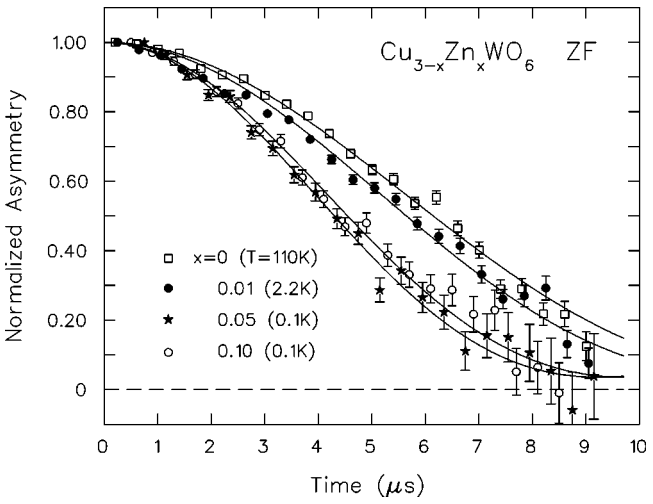

FIG. 11. ZF-μSR spectra of polycrystalline $Cu_{3-x}Zn_xWO_6$ at low temperatures. The ZF spectra of pure Cu_3WO_6 at $T = 110$ K is also included for comparison.

small at very low temperature, and thus there is no sign of critical slowing down nor phase transition of electron spins. We note that the depolarization rate is slightly increased with increasing Zn-concentration x. We would rather expect the reduction of the depolarization rate by Zn substitution because Zn has no nuclear spin ($I = 0$) while Cu has $I = 3/2$ and because Zn^{2+} has larger ionic radius than Cu^{2+}. The origin of this effect is unclear at this moment. Fully polarized spectra in LF of 100 G at $T = 2.0$ K confirm the absence of critical slowing down and/or phase transition in the doped compound at low temperatures.

V. DISCUSSION

Nonmagnetic ground states of quasi-1D systems, such as $CuGeO_3$(Refs. 5,6) and $SrCu_2O_3$,[7] are usually altered to antiferromagnetic order by slight magnetic dilution. Recently, hole-induced long-range order was also discovered in a new Haldane system $PbNi_2V_2O_8$.[19] Quasistatic spin freezing in a

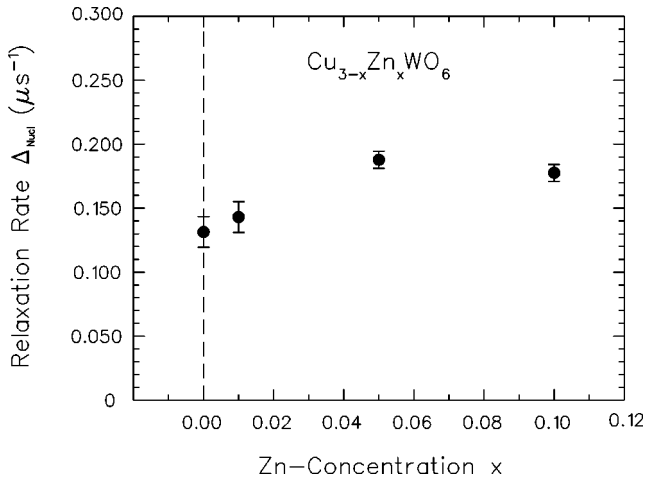

FIG. 12. Zn concentration x versus depolarization rate $\Delta_{\rm nucl}$ defined in Eq. (15).

spin-ring system Cu_3WO_6, and its suppression by Zn doping is quite peculiar compared to the above examples of 1D spin systems. On the other hand, static spin freezing behavior has been detected by μSR in other widely accepted spin gap systems, such as a plaquette spin system CaV_4O_9(Ref. 20) and a zig-zag chain system $KCuCl_3$.[21] Remarkable similarities to the present case are found in the μSR results of the charge-ordered system $Na_xV_2O_5$.[4] Pure NaV_2O_5 has a spin-ladder structure, and is thought to undergo a charge-order transition at $T_c=35$ K from a state of a mixed valence of Vanadium ions $V^{4.5+}$ above T_c to a localization of d electrons to form a spin-singlet below T_c. A gap energy in susceptibility is suppressed in a charge-doped system ($x<1$).[22] Quasistatic spin freezing at 11 K has been detected by μSR in the pure system ($x=1$) while the freezing is suppressed in the charge-doped system ($x<1$).[23] The magnetic behavior of pure and charge-doped NaV_2O_5 detected by μSR is very similar to that of Cu_3WO_6.

The observed energy gap in susceptibility and neutron scattering measurements strongly supports a singlet ground state in Cu_3WO_6. The gap energy $E_g\sim44.6$ K is much larger than the freezing temperature $T_f=7.0$ K, which indicates the existence of two distinct electron systems. Thus, it is probable that part of the spin system forms a spin-singlet state while the remainder undergo spin freezing below T_f. As Zn^{2+} are doped, some holes cut the spin-ring and leave it as a finite spin chain. Spins within a finite chain are generally expected to fluctuate without any spatial correlations to each other, which can lead to a disappearance of the gap energy observed in the susceptibility. These fluctuations then induce fluctuations of the spins corresponding to the freezing spins in the undoped compound.

The magnetically inequivalent muon environments observed in the ZF spectra below T_f could be attributed to two kinds of the spin states at low temperature as proposed above. Let us consider several scenarios of the two different spin states. If active nonsinglet Cu spins exist over the volume in a way similar to dilute alloy spin glasses, we expect that the internal field at the muon sites would have Lorentzian distribution over the entire volume. In this case, we can not expect division of muon environment into two different groups. Moreover, the Curie term in the susceptibility of our specimen corresponds to 0.0663% of free spin-1/2 moments (Table I), which could create only $\sim$0.5 G of internal field,[14,24] while the observed static field is $H_{\rm int}\sim30$ G. Therefore, we can disregard the possibility that the isolated $S=1/2$ impurities undergo spin freezing in a way similar to dilute alloy spin glasses. The existence of two different magnetic environments, with the better fittings of the line shape to exponential distribution which describes the field distribution for magnetic clusters with spatially varying frozen moment size, indicates that the spin freezing occurs in such magnetic clusters which occupy about a half of the volume fraction of the sample. The freezing state of Cu_3WO_6 may resemble the ordered state of spin-ladder $SrCu_2O_3$, in which an $S=1/2$ spin liberated by impurity and/or (Cu,Zn) substitution can be shared by many Cu moments.[7,25] This could result in a large effect for muon internal field, yet with quite a small effect in susceptibility.

The possibility of a muon-induced effect was proposed to explain the spin-glass-like behavior in $KCuCl_3$.[26] In that study it was postulated that the presence of the μ^+ could destroy singlet pairs and those liberated spins develop a quasistatic behavior in part of volume, while relatively slow fluctuations persist in the remaining volume. Similar muon-induced static freezing is also proposed for organic spin-Peierls MEM(TCNQ)$_2$.[27] These muon effects are analogous to an effect of (Ge,Si) substitution in $CuGeO_3$.[28,29] The presence of a positive charge (μ^+) could cause local strain to perturb the lattice, prevent spin-singlet formations, and induce static freezing of spins around μ^+. In μSR experiments not more than one muon is allowed to be in a specimen at a time. Therefore, even when a muon perturbs its surroundings, the existence of μ^+ cannot induce any many-body process. If the correlation time of unpaired spins around μ^+ becomes slower than 10^{-6} s, those spins would look static to μ^+. This case cannot de distinguished from many-body spin freezing.

We shall note, however, that in undoped $CuGeO_3$,[30] Y_2BaNiO_5,[31] and $SrCu_2O_3$,[15,32] we did not find evidence of spin freezing by μSR. These three systems exhibit spin freezing by magnetic dilution and/or charge doping with a very small impurity concentration. Furthermore, μSR measurements in such doped systems found spin freezing temperature consistent with the results from susceptibility measurements. These features clearly demonstrate absence of muon-induced effects in these three representative spin gap systems. Further studies with other nonperturbing magnetic probes, such as neutron scattering, NMR and ac susceptibility, are necessary to clarify this aspect.

VI. CONCLUSIONS

Magnetic properties of the pure and doped spin-ring system $Cu_{3-x}Zn_xWO_6$ were studied utilizing the μSR technique. Quasistatic spin freezing is observed below $T_f=7.0$ K in pure Cu_3WO_6 in contrast to the previous neutron scattering and susceptibility studies in which an energy gap was observed. Zn-doped $Cu_{3-x}Zn_xWO_6$ with $x=0.01$, 0.05, and 0.10, however, exhibit no signatures of spin freezing down to $T=2.20$, 0.1, and 0.1 K, respectively. The μSR results of $Cu_{3-x}Zn_xWO_6$ are similar to those of a charge-ordered system $Na_xV_2O_5$, where we have also observed static spin freezing in an apparently gapped pure system ($x=1$) and the suppression of the freezing in a charge-doped system ($x<1$). Although additional measurements are necessary to confirm the observed spin freezing, as well as to investigate a possibility of muon-induced effect on spin-gap systems, available μSR results favor a picture of static spin freezing in Cu_3WO_6.

ACKNOWLEDGMENTS

This work was supported financially by NEDO (International Joint Research Grant) from Japan, and NSF (Grant Nos. DMR-95-10453, 10454, 98-02000, and 01-02752) from U.S.A.

*Present address: Superconductivity Research Laboratory, ISTEC, 1-10-13 Shinonome, Koto-ku, Tokyo 135-0062, Japan.

[1] M. Hase, I. Terasaki, and K. Uchinokura, Phys. Rev. Lett. **70**, 3651 (1993).

[2] M. Azuma, Z. Hiroi, M. Takano, K. Ishida, and Y. Kitaoka, Phys. Rev. Lett. **73**, 3463 (1994).

[3] D.J. Buttrey, J.D. Sullivan, and A.L. Rheingold, J. Solid State Chem. **88**, 291 (1990).

[4] M. Isobe and Y. Ueda, J. Phys. Soc. Jpn. **65**, 1178 (1996).

[5] M. Hase, I. Terasaki, Y. Sasago, K. Uchinokura, and H. Obara, Phys. Rev. Lett. **71**, 4059 (1993).

[6] K. Manabe, H. Ishimoto, N. Koide, Y. Sasago, and K. Uchinokura, Phys. Rev. B **58**, R575 (1998).

[7] M. Azuma, Y. Fujishiro, M. Takano, M. Nohara, and H. Takagi, Phys. Rev. B **55**, R8658 (1997).

[8] M. Uehara, T. Nagata, J. Akimitsu, H. Takahashi, N. Mori, and K. Kinoshita, J. Phys. Soc. Jpn. **65**, 2764 (1996).

[9] E. Gebert and L. Kihlborg, Acta Chem. Scand. **23**, 221 (1969).

[10] M. Hase and K. Uchinokura, Physica B **215**, 325 (1995).

[11] J.C. Bonner and M.E. Fisher, Phys. Rev. A **135**, A640 (1964).

[12] M. Hase, Y. Sasago, K. Uchinokura, K. Hirota, and G. Shirane, J. Phys. Soc. Jpn. **65**, 372 (1996).

[13] R.S. Hayano, Y.J. Uemura, J. Imazato, N. Nishida, T. Yamazaki, and R. Kubo, Phys. Rev. B **20**, 850 (1979).

[14] Y.J. Uemura, T. Yamazaki, D.R. Harshman, M. Senba, and E.J. Ansaldo, Phys. Rev. B **31**, 546 (1985).

[15] M.I. Larkin, Y. Fudamoto, I.M. Gat, A. Kinkhabwala, K.M. Kojima, G.M. Luke, J. Merrin, B. Nachumi, Y.J. Uemura, M. Azuma, T. Saito, and M. Takano, Phys. Rev. Lett. **85**, 1982 (2000).

[16] M.I. Larkin, Y. Fudamoto, I.M. Gat, A. Kinkhabwala, K.M. Kojima, G.M. Luke, J. Merrin, B. Nachumi, Y.J. Uemura, M. Azuma, and M. Takano, Physica B **289-290**, 153 (2000).

[17] The field dependence of λ for an exponential field distribution is given as $\lambda = 4\delta^2\nu/[\nu^2 + (\gamma_\mu H_L)^2]$; M. I. Larkin (unpublished).

[18] M. Azuma, M. Takano, and R.S. Eccleston, J. Phys. Soc. Jpn. **67**, 740 (1998).

[19] Y. Uchiyama, Y. Sasago, I. Tsukada, K. Uchinokura, A. Zheludev, T. Hayashi, N. Miura, and P. Böni, Phys. Rev. Lett. **83**, 632 (1999).

[20] G.M. Luke, Y. Fudamoto, M.J.P. Gingras, K.M. Kojima, M. Larkin, J. Merrin, B. Nachumi, and Y.J. Uemura, J. Magn. Magn. Mater. **177-181**, 754 (1998).

[21] W. Higemoto, H. Tanaka, I. Watanabe, and K. Nagamine, Phys. Lett. A **243**, 80 (1998).

[22] M. Isobe and Y. Ueda, J. Alloys Compd. **262-263**, 180 (1997).

[23] Y. Fudamoto, K.M. Kojima, M.I. Larkin, G.M. Luke, J. Merrin, B. Nachumi, Y.J. Uemura, M. Isobe, and Y. Ueda, Phys. Rev. Lett. **83**, 3301 (1999).

[24] V. Cannella and J.A. Mydosh, Phys. Rev. B **6**, 4220 (1972).

[25] H. Fukuyama, N. Nagaosa, M. Saito, and T. Tanimoto, J. Phys. Soc. Jpn. **65**, 2377 (1996).

[26] D. Andreika, N. Cavadini, H.U. Güdel, F.N. Gygax, K. Krämer, M. Pinkpank, and A. Schenck, Physica B **289-290**, 176 (2000).

[27] B.W. Lovett, S.J. Blundell, F.L. Pratt, T. Jestädt, W. Hayes, H. Takagi, and M. Kurmoo, Physica B **289-290**, 145 (2000).

[28] J.P. Renard, K. Le Dang, P. Vellet, G. Dhalenne, A. Revcolevschi, and L.P. Regnault, Europhys. Lett. **30**, 475 (1995).

[29] H. Fukuyama, T. Tanimoto, and M. Saito, J. Phys. Soc. Jpn. **65**, 1182 (1996).

[30] K.M. Kojima, Y. Fudamoto, M. Larkin, G.M. Luke, J. Merrin, B. Nachumi, Y.J. Uemura, M. Hase, Y. Sasago, K. Uchinokura, Y. Ajiro, A. Revcolevschi, and J.P. Renard, Phys. Rev. Lett. **79**, 503 (1997).

[31] K. Kojima, A. Keren, L.P. Le, G.M. Luke, B. Nachumi, W.D. Wu, Y.J. Uemura, K. Kiyono, S. Miyasaka, H. Takagi, and S. Uchida, Phys. Rev. Lett. **74**, 3471 (1995).

[32] K.M. Kojima, Y. Fudamoto, M. Larkin, G.M. Luke, J. Merrin, B. Nachumi, Y.J. Uemura, N. Motoyama, H. Eisaki, S. Uchida, K. Yamada, Y. Endoh, S. Hosoya, B.J. Sternlieb, and G. Shirane, Phys. Rev. Lett. **78**, 1787 (1997).